

This article is published as part of the *Dalton Transactions* themed issue entitled:

## New Talent

*Showcasing the strength of research being carried out by tomorrow's leaders in the field of inorganic chemistry*

Guest Editor Polly Arnold  
University of Edinburgh, UK

Published in [issue 2, 2010](#) of *Dalton Transactions*



Image reproduced with permission of Mark Muldoon

Articles in the issue include:

### **PERSPECTIVES:**

[Modern multiphase catalysis: new developments in the separation of homogeneous catalysts](#)

Mark J. Muldoon, *Dalton Trans.*, 2010, DOI: 10.1039/b916861n

[Probing bioinorganic chemistry processes in the bloodstream to gain new insights into the origin of human diseases](#)

Elham Zeini Jahromi and Jürgen Gailer, *Dalton Trans.*, 2010, DOI: 10.1039/b912941n

### **COMMUNICATIONS:**

[Facile entry to 3d late transition metal boryl complexes](#)

Ba L. Tran, Debashis Adhikari, Hongjun Fan, Maren Pink and Daniel J. Mindiola, *Dalton Trans.*, 2010, DOI: 10.1039/b912040h

[Probing the kinetics of ligand exchange on colloidal gold nanoparticles by surface-enhanced raman scattering](#)

Yuhua Feng, Shuangxi Xing, Jun Xu, Hong Wang, Jun Wei Lim and Hongyu Chen, *Dalton Trans.*, 2010, DOI: 10.1039/b912317b

Visit the *Dalton Transactions* website for more cutting-edge inorganic and organometallic research  
[www.rsc.org/dalton](http://www.rsc.org/dalton)

# Chelating tris(amidate) ligands: versatile scaffolds for nickel(II)†

Matthew B. Jones,<sup>a</sup> Brian S. Newell,<sup>b</sup> Wesley A. Hoffert,<sup>b</sup> Kenneth I. Hardcastle,<sup>a</sup> Matthew P. Shores<sup>b</sup> and Cora E. MacBeth<sup>\*a</sup>

Received 16th July 2009, Accepted 15th October 2009

First published as an Advance Article on the web 17th November 2009

DOI: 10.1039/b914301g

The synthesis and characterization of nickel complexes supported by a family of open-chain, tetradentate, tris(amidate) ligands,  $[\text{N}(o\text{-PhNC}(\text{O})\text{R})_3]^{3-}$  ( $[\text{L}^{\text{R}}]^{3-}$  where  $\text{R} = \text{}^i\text{Pr}$ ,  $\text{}^t\text{Bu}$ , and  $\text{Ph}$ ) is described. The complexes  $[\text{Ni}(\text{L}^{\text{iPr}})]^-$ ,  $[\text{Ni}(\text{L}^{\text{tBu}})]^-$ , and  $[\text{Ni}(\text{L}^{\text{Ph}})(\text{CH}_3\text{CN})]^-$  have been characterized by solution-state spectroscopic methods and single crystal X-ray diffraction. Each ligand gives rise to a different primary coordination sphere about the nickel centre. These studies indicate that the ligands' acyl substituents can be used to regulate the coordination mode of the amidate donors to nickel and the coordination number of the nickel centres. In addition, the ability of these complexes to bind cyanide has been explored. These experiments demonstrate that only one of these complexes,  $[\text{Ni}(\text{L}^{\text{iPr}})]^-$ , is able to irreversibly bind cyanide and can be used to assemble  $[\text{Et}_4\text{N}]_3[\text{Ni}(\text{L}^{\text{iPr}})(\mu_2\text{-CN})\text{Co}(\text{L}^{\text{iPr}})]$ , a cyanide bridged, heterobimetallic complex. The synthesis and characterization of the cyanide containing complexes, including magnetic susceptibility studies, are described.

## Introduction

Nickel complexes supported by amidate-based ligand systems have been used to investigate the role of nickel in biological systems<sup>1-9</sup> and observe high-valent nickel species.<sup>9-18</sup> The majority of these studies have employed either macrocyclic<sup>9-11</sup> or open-chain chelating ligands<sup>1-5,12-16</sup> that stabilize Ni(II) ions in square planar coordination geometries. Open-chain ligands that contain amidate donors and stabilize Ni(II) ions in alternative coordination geometries have received less attention but have been used to prepare nickel complexes that display unique coordination geometries (*i.e.*, trigonal pyramidal<sup>17-19</sup>) and biomimetic reactivities.<sup>7,8</sup>

Ligand systems that incorporate amidate donors are attractive scaffolds for several reasons: (1) The amide functional group ( $[\text{RNHC}(\text{O})\text{R}']$ ) is readily synthesized in high yields from amine precursors, making ligands of this type highly modular. (2) Substituents on amide-based ligands can be varied to regulate both electronic and steric features of the resulting transition metal complexes.<sup>17,20-25</sup> (3) Amide functional groups are chemically robust. However, a significant challenge in the application of these ambidentate ligands to metal complex design is to control the binding mode (Chart 1) so as to afford predictable coordination geometries.<sup>20</sup>

Given the modular nature of open-chain amidate ligands, our laboratory has been exploring the coordination chemistry of tris(amidate) ligand systems ( $[\text{N}(o\text{-PhNC}(\text{O})\text{R})_3]^{3-}$ ) derived from the tris(2-aminophenyl)amine ( $\text{N}(o\text{-PhNH}_2)_3$ ) ligand scaffold. We have demonstrated that these systems, which incorporate *ortho*-

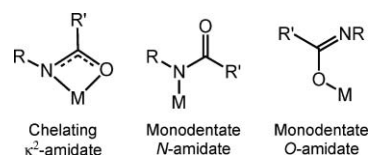


Chart 1 Possible coordination modes of amidate donors.

substituted phenylene units into the ligand backbone, can be used to stabilize metals with unique structural properties.<sup>26,27</sup> These studies suggested that the ligand's acyl substituents could be used to regulate exogenous anion binding<sup>26</sup> and, in the case of Al(III) complexes,<sup>27</sup> enforce mononuclear complex formation.

Herein, we report the synthesis and characterization of nickel complexes supported by a series of these tris(amidate) ligands ( $[\text{N}(o\text{-PhNC}(\text{O})\text{R})_3]^{3-}$ ,  $\text{R} = \text{}^i\text{Pr}$ ,  $\text{}^t\text{Bu}$ , and  $\text{Ph}$ ) and demonstrate that the ligands' amidate acyl substituents can be used to control both the coordination number of the nickel ion and the coordination mode (Chart 1) of the amidate donors in the resulting metal complexes. In addition, we describe the ability of these nickel complexes to bind cyanide and show that, in one case, complexes of this type can be used to assemble a heterobimetallic complex.

## Results and discussion

### Synthesis

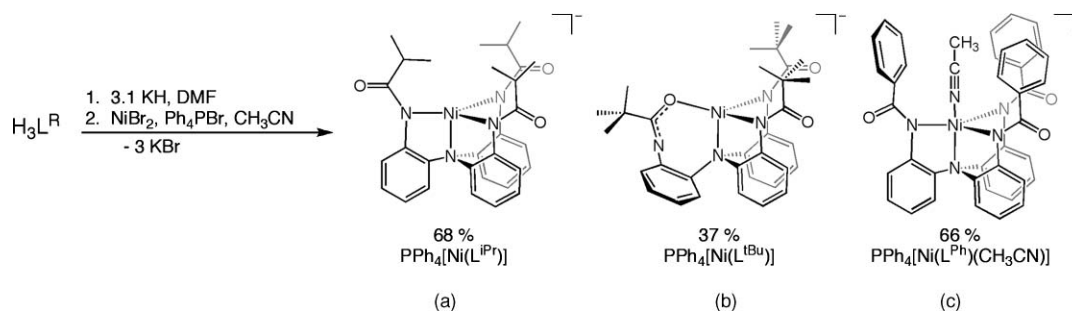
The syntheses of the ligands  $\text{H}_3\text{L}^{\text{iPr}}$  ( $\text{H}_3\text{L}^{\text{iPr}} = \text{N}(o\text{-PhNHC}(\text{O})^i\text{Pr})_3$ ) and  $\text{H}_3\text{L}^{\text{tBu}}$  ( $\text{H}_3\text{L}^{\text{tBu}} = \text{N}(o\text{-PhNHC}(\text{O})^t\text{Bu})_3$ ) have been recently reported.<sup>26,27</sup> The phenyl derivative,  $\text{H}_3\text{L}^{\text{Ph}}$  ( $\text{H}_3\text{L}^{\text{Ph}} = \text{N}(o\text{-PhNHC}(\text{O})\text{Ph})_3$ ), is prepared in good yield (85%) using an analogous synthetic strategy (see Experimental section for complete details).

The nickel complexes  $\text{PPh}_4[\text{Ni}(\text{L}^{\text{iPr}})]$ ,  $\text{PPh}_4[\text{Ni}(\text{L}^{\text{tBu}})]$ , and  $\text{PPh}_4[\text{Ni}(\text{L}^{\text{Ph}})(\text{CH}_3\text{CN})]$  are synthesized using the general route outlined in Scheme 1. In a typical preparation, the ligand is reacted with a slight excess (3.1 equivalents) of a metal

<sup>a</sup>Department of Chemistry, Emory University, Atlanta, GA, USA. E-mail: cmacbet@emory.edu; Fax: 01 404-727-6586; Tel: 01-404-727-7033

<sup>b</sup>Department of Chemistry, Colorado State University, Fort Collins, CO, USA. E-mail: shores@lamar.colostate.edu; Tel: 01-970-491-7235

† Electronic supplementary information (ESI) available: Crystallographic data for all complexes, electrochemistry, and additional magnetic data and fits. CCDC reference numbers 738758–738762. For ESI and crystallographic data in CIF or other electronic format see DOI: 10.1039/b914301g



**Scheme 1** General synthetic preparation of (A)  $\text{PPh}_4[\text{Ni}(\text{L}^{\text{iPr}})]$ , (B)  $\text{PPh}_4[\text{Ni}(\text{L}^{\text{tBu}})]$ , and (C)  $\text{PPh}_4[\text{Ni}(\text{L}^{\text{Ph}})(\text{CH}_3\text{CN})]$ .

**Table 1** Selected bond lengths (Å) and angles ( $^\circ$ ) for  $[\text{Ni}(\text{L}^{\text{iPr}})]^-$ ,  $[\text{Ni}(\text{L}^{\text{tBu}})]^-$ , and  $[\text{Ni}(\text{L}^{\text{Ph}})]^-$

	$[\text{Ni}(\text{L}^{\text{iPr}})]^-$	$[\text{Ni}(\text{L}^{\text{tBu}})]^-$	$[\text{Ni}(\text{L}^{\text{Ph}})]^-$
Ni–N1	2.0189(15)	2.043(2)	2.080(3)
Ni–N2	1.9542(15)	1.976(2)	2.078(3)
Ni–N3	1.9570(16)	2.009(2)	2.056(3)
Ni–N4	1.9493(16)		2.039(3)
Ni–N5			2.012(3)
Ni–O3		1.9167(19)	
N1–Ni–N2	86.32(6)	84.25(9)	79.33(12)
N1–Ni–N3	85.39(7)	82.16(9)	80.01(11)
N1–Ni–N4	84.85(7)		80.13(12)
N1–Ni–O3		102.78	
N1–Ni–N5			175.14(13)
N2–Ni–N3	112.68(7)	110.16(9)	112.35(13)
N2–Ni–N4	127.19(7)		124.93(13)
N3–Ni–N4	118.29(7)		113.45(12)
Ni–N5–C40			170.4(4)

hydride and transmetalated *in situ* with  $\text{NiBr}_2$ . These steps yield the corresponding potassium salts of the metal complexes (e.g.,  $\text{K}[\text{Ni}(\text{L}^{\text{iPr}})]$ ) and two equivalents of the  $\text{KBr}$  by-product. The potassium salts are isolable but difficult to crystallize. However, *in situ* salt metathesis with tetraphenylphosphonium bromide ( $[\text{PPh}_4]\text{Br}$ ) readily affords the tetraphenylphosphonium salts (e.g.,  $\text{PPh}_4[\text{Ni}(\text{L}^{\text{iPr}})]$ ) in reasonable yields (Scheme 1). For each complex, the tetraphenylphosphonium salt and potassium salt exhibit nearly identical spectroscopic (IR, UV-visible absorption, and  $^1\text{H}$  NMR) signatures, indicating the counter cation is not significantly altering the coordination mode of the ligand. The tetraphenylphosphonium salts can be recrystallized to produce analytically pure materials.

### Structural characterization

The nickel complexes  $\text{PPh}_4[\text{Ni}(\text{L}^{\text{iPr}})]$ ,  $\text{PPh}_4[\text{Ni}(\text{L}^{\text{tBu}})]$ , and  $\text{PPh}_4[\text{Ni}(\text{L}^{\text{Ph}})(\text{CH}_3\text{CN})]$  have been characterized by single-crystal X-ray diffraction. The molecular structures of these complexes are illustrated in Fig. 1 and selected bond lengths and angles are given in Table 1. Crystallographic data and refinement parameters are listed in Table 2.

The  $\text{Ni}(\text{II})$  ion in  $[\text{Ni}(\text{L}^{\text{iPr}})]^-$  possesses a distorted trigonal pyramidal coordination geometry. The nickel centre is coordinated by the three *N*-amidate donors, which make up the equatorial plane, and the tertiary amine donor of the ligand backbone (Fig. 1A). Together these donors form three five-membered chelate rings about the nickel ion. The complex displays  $\text{Ni}-\text{N}_{\text{amidate}}$  bond lengths of 1.9542(15), 1.9570(16), and 1.9493(16) Å and a

$\text{Ni}-\text{N}_{\text{amine}}$  bond length of 2.0189(15) Å. The  $\text{N}_{\text{amidate}}-\text{Ni}-\text{N}_{\text{amidate}}$  bond angles (127.19(7), 118.29(7), and 112.68(7) $^\circ$ ) are close to the idealized value of 120 $^\circ$  expected for a perfect trigonal pyramid. The nickel ion rises ~0.15 Å above the equatorial plane defined by the three *N*-amidate donors toward the vacant axial coordination site. The isopropyl substituents of the ligand are positioned above the equatorial plane so that they completely surround this open axial coordination site. This type of arrangement has been observed in other nickel complexes supported by open-chain tris(amidate) ligands.<sup>17,18</sup>

The geometry of four-coordinate metal centres can be quantitatively evaluated using the  $\tau_4$  parameter recently described by Houser and co-workers.<sup>28</sup> This parameter is useful, as the extreme values of 0.0 and 1.0 correspond to idealized tetrahedral and square planar geometries, respectively, and idealized intermediate geometries (seesaw and trigonal pyramidal) fall between these two values. The  $\tau_4$  value of 0.82 exhibited by  $[\text{Ni}(\text{L}^{\text{iPr}})]^-$  is close to the idealized  $\tau_4$  value expected for an idealized trigonal pyramidal complex (0.85).

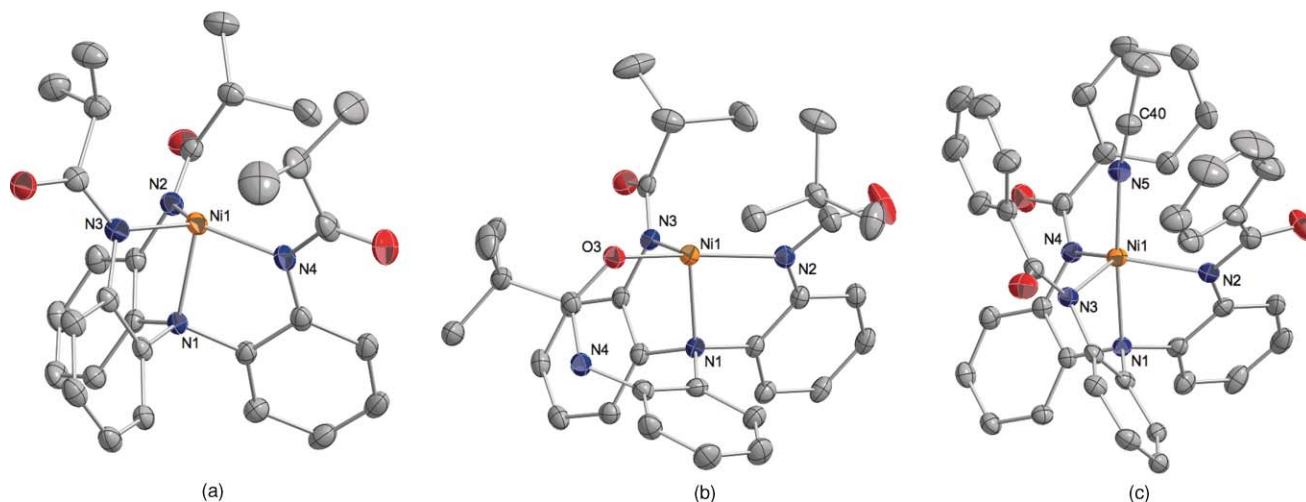
Unlike the nickel ion in  $[\text{Ni}(\text{L}^{\text{iPr}})]^-$ , the equatorial plane about the nickel centre in  $[\text{Ni}(\text{L}^{\text{tBu}})]^-$  (Fig. 1B) consists of two *N*-amidate donors and one *O*-amidate donor. The two coordinated *N*-amidate donors are positioned so that their *tert*-butyl substituents are significantly shielding the nickel centre. The third arm of the ligand coordinates through an *O*-amidate donor, which results in the formation of a seven-membered chelate ring within the complex. This coordination mode positions the *tert*-butyl substituent of the *O*-amidate donor a greater distance from the nickel centre, reducing steric strain. The bond lengths of the NCO moiety (N–C 1.290(4) and C–O 1.302(3) Å) comprising the *O*-amidate donor indicate that the anionic charge is delocalized throughout this unit. In this coordination environment, the nickel ion is nearly coplanar with the equatorial donors and deviates only 0.032 Å from the plane.

The overall geometry is distorted trigonal pyramidal ( $\tau_4 = 0.71$ ). The  $\text{Ni}-\text{N}_{\text{amidate}}$  bond lengths (1.976(2) and 2.009(2) Å) in  $[\text{Ni}(\text{L}^{\text{tBu}})]^-$  are longer than the  $\text{Ni}-\text{N}_{\text{amidate}}$  bond lengths observed in  $[\text{Ni}(\text{L}^{\text{iPr}})]^-$  (Table 1). The  $\text{Ni}-\text{O}_{\text{amidate}}$  bond length in  $[\text{Ni}(\text{L}^{\text{tBu}})]^-$  is the shortest bond within the nickel centre's primary coordination sphere (1.9167(19) Å).

In contrast to both  $[\text{Ni}(\text{L}^{\text{iPr}})]^-$  and  $[\text{Ni}(\text{L}^{\text{tBu}})]^-$ , in which the nickel ions are four-coordinate 16  $e^-$  species, the nickel complex of the  $[\text{L}^{\text{Ph}}]^-$  ligand is isolated as an 18  $e^-$ , five-coordinate complex,  $[\text{Ni}(\text{L}^{\text{Ph}})(\text{CH}_3\text{CN})]^-$  with a coordinated acetonitrile ligand (Fig. 1C). The  $\text{Ni}-\text{N}_{\text{amidate}}$  bond lengths of 2.078(3), 2.056(3), and 2.039(3) Å exhibited by  $[\text{Ni}(\text{L}^{\text{Ph}})(\text{CH}_3\text{CN})]^-$  are all longer than

**Table 2** Crystallographic data for  $[\text{Ni}(\text{L}^{\text{iPr}})]^-$ ,  $[\text{Ni}(\text{L}^{\text{iBu}})]^-$ ,  $[\text{Ni}(\text{L}^{\text{Ph}})]^-$ ,  $[\text{Ni}(\text{L}^{\text{iPr}})(\text{CN})]^{2-}$ , and  $[\text{NiCo}(\text{L}^{\text{iPr}})_2(\text{CN})]^{3-}$ 

	$\text{PPh}_4[\text{Ni}(\text{L}^{\text{iPr}})] \cdot 2\text{DMF}$	$\text{PPh}_4[\text{Ni}(\text{L}^{\text{iBu}})] \cdot \text{DMF} \cdot 0.6\text{Et}_2\text{O}$	$\text{PPh}_4[\text{Ni}(\text{L}^{\text{Ph}})(\text{CH}_3\text{CN})] \cdot 2\text{CH}_3\text{CN}$	$[\text{Et}_4\text{N}]_2[\text{Ni}(\text{L}^{\text{iPr}})(\text{CN})]$	$[\text{Et}_4\text{N}]_3[\text{NiCo}(\text{L}^{\text{iPr}})_2(\text{CN})]$
Empirical formula	$\text{C}_{60}\text{H}_{67}\text{N}_6\text{NiO}_5\text{P}$	$\text{C}_{62.40}\text{H}_{72}\text{N}_5\text{NiO}_{4.6}\text{P}$	$\text{C}_{69}\text{H}_{56}\text{N}_7\text{NiO}_3\text{P}$	$\text{C}_{47}\text{H}_{73}\text{N}_7\text{NiO}_3$	$\text{C}_{85}\text{H}_{126}\text{CoN}_{12}\text{NiO}_6$
Crystal system	Triclinic	Triclinic	Monoclinic	Monoclinic	Rhombohedral
Space group	$P\bar{1}$	$P\bar{1}$	$P2_1/c$	$P2_1/n$	$R\bar{3}$
$a/\text{\AA}$	11.3871(1)	14.4575(8)	10.9218(3)	11.412(6)	19.0019(17)
$b/\text{\AA}$	16.0284(2)	15.1016(8)	25.9666(9)	18.653(10)	19.0019(17)
$c/\text{\AA}$	16.8718(2)	15.4786(8)	20.1405(7)	43.91(2)	21.787(4)
$\alpha$ (°)	115.3630(10)	64.786(3)	90	90	90
$\beta$ (°)	102.2640(10)	72.689(3)	90.153(17)	96.676(14)	90
$\gamma$ (°)	91.6840(10)	77.867(3)	90	90	120
$V/\text{\AA}^3$	2693.69(5)	2905.3(3)	5711.9(3)	9285(8)	6812.7(15)
$Z$	2	2	4	8	3
Crystal size/mm	$0.50 \times 0.32 \times 0.30$	$0.52 \times 0.40 \times 0.18$	$0.33 \times 0.26 \times 0.20$	$0.42 \times 0.20 \times 0.15$	$0.13 \times 0.13 \times 0.05$
$T/\text{K}$	173(2)	173(2)	173(2)	172(2)	172(2)
Reflections collected	39239	42454	60804	159728	41833
Indep. reflns ( $R_{\text{int}}$ )	10982 (0.0400)	11735 (0.0581)	10176 (0.0786)	11486 (0.0843)	8677 (0.0971)
Goodness-of-fit on $F^2$	1.036	1.041	1.021	1.056	1.021
Final $R$ indices [ $I > 2\sigma(I)$ ]	$R_1 = 0.0438$ $wR_2 = 0.1162$	$R_1 = 0.0505$ $wR_2 = 0.1414$	$R_1 = 0.0673$ $wR_2 = 0.1795$	$R_1 = 0.0793$ $wR_2 = 0.1873$	$R_1 = 0.0733$ $wR_2 = 0.1488$
$R$ indices (all data)	$R_1 = 0.0519$ $wR_2 = 0.1221$	$R_1 = 0.0745$ $wR_2 = 0.1633$	$R_1 = 0.1053$ $wR_2 = 0.1910$	$R_1 = 0.0925$ $wR_2 = 0.1954$	$R_1 = 0.1447$ $wR_2 = 0.1663$

**Fig. 1** Thermal ellipsoid diagrams of (A)  $[\text{Ni}(\text{L}^{\text{iPr}})]^-$ , (B)  $[\text{Ni}(\text{L}^{\text{iBu}})]^-$ , and (C)  $[\text{Ni}(\text{L}^{\text{Ph}})(\text{CH}_3\text{CN})]^-$  drawn at 35% probability. Hydrogen atoms and counter cations have been removed for clarity.

the Ni– $\text{N}_{\text{amidate}}$  bond lengths observed in  $[\text{Ni}(\text{L}^{\text{iPr}})]^-$  and  $[\text{Ni}(\text{L}^{\text{iBu}})]^-$  (Table 1). In addition, the  $\text{N}_{\text{amine}}\text{--Ni}$  bond length (2.080 Å) in  $[\text{Ni}(\text{L}^{\text{Ph}})(\text{CH}_3\text{CN})]^-$  is longer than the  $\text{N}_{\text{amine}}\text{--Ni}$  bond lengths observed in the four-coordinate species, presumably due to the *trans* influence exerted by the acetonitrile ligand. The  $\text{N}_{\text{amine}}\text{--Ni--N}_{\text{NCCH}_3}$  bond angle is nearly linear (175.14(13)°) allowing the phenyl substituents of the ligand to orient about the coordinated acetonitrile in a bowl-like cavity structure.

Taken together, these structural data suggest that the relative size of the ligands' amidate acyl substituents can significantly influence both the coordination mode of the ligand and the coordination number of the resulting transition metal complexes. To further probe this trend, attempts were made to synthesize the methyl congener of this series using the  $\text{H}_3\text{L}^{\text{Me}}$  ligand (where  $[\text{H}_3\text{L}^{\text{Me}}] = \text{N}(\text{o-PhNHC}(\text{O})\text{CH}_3)_3$ ). Unfortunately, these experiments led only to complicated reaction mixtures. We have observed similar results when attempting to prepare aluminium-containing analogues.<sup>27</sup>

Specifically, hexacoordinate, mononuclear tris( $\kappa^2$ -amidate) aluminium(III) complexes were isolated and characterized with both the  $[\text{L}^{\text{iPr}}]^{3-}$  and  $[\text{L}^{\text{iBu}}]^{3-}$  ligands. However, attempts to isolate the analogous complex using the methyl ligand derivative,  $[\text{L}^{\text{Me}}]^{3-}$ , were unsuccessful and lead only to the formation of multinuclear species. These results suggest that larger acyl substituents are required to ensure the formation of mononuclear complexes with these ligands.

### Spectroscopic characterization

The nickel complexes have been characterized by  $^1\text{H}$  NMR, FT-IR, and UV-visible absorption spectroscopies. All three complexes ( $[\text{Ni}(\text{L}^{\text{iPr}})]^-$ ,  $[\text{Ni}(\text{L}^{\text{iBu}})]^-$ , and  $[\text{Ni}(\text{L}^{\text{Ph}})(\text{CH}_3\text{CN})]^-$ ) exhibit paramagnetically-shifted  $^1\text{H}$  NMR spectra. The  $^1\text{H}$  NMR (25 °C,  $\text{CD}_3\text{CN}$ ) spectra of  $[\text{Ni}(\text{L}^{\text{iPr}})]^-$  and  $[\text{Ni}(\text{L}^{\text{Ph}})(\text{CH}_3\text{CN})]^-$  are indicative of pseudo  $C_3$ -symmetric species in solution (see Experimental

section). In contrast, the spectrum of  $[\text{Ni}(\text{L}^{\text{tBu}})]^-$ , under identical experimental conditions is significantly more complicated, exhibiting seventeen paramagnetically-shifted resonances consistent with a lower symmetry ( $C_1$ ) species. Variable temperature ( $-60$  to  $30^\circ\text{C}$ )  $^1\text{H}$  NMR spectroscopy was conducted on both  $[\text{Ni}(\text{L}^{\text{iPr}})]^-$  and  $[\text{Ni}(\text{L}^{\text{tBu}})]^-$  in  $d_6$ -acetone and confirmed non-fluxional solution-state behaviour of these species over this range of temperatures.

The magnetic moments of  $[\text{Ni}(\text{L}^{\text{iPr}})]^-$ ,  $[\text{Ni}(\text{L}^{\text{tBu}})]^-$ , and  $[\text{Ni}(\text{L}^{\text{Ph}})(\text{CH}_3\text{CN})]^-$  were obtained using solution phase  $^1\text{H}$  NMR methods.<sup>29,30</sup> The four-coordinate species,  $[\text{Ni}(\text{L}^{\text{iPr}})]^-$  and  $[\text{Ni}(\text{L}^{\text{tBu}})]^-$ , exhibit  $\mu_{\text{eff}}$  values of 3.03 and 3.37  $\mu_{\text{B}}$ , respectively, indicative of  $S = 1$  ground states. The five-coordinate  $[\text{Ni}(\text{L}^{\text{Ph}})(\text{CH}_3\text{CN})]^-$  exhibits a  $\mu_{\text{eff}}$  value of 3.27  $\mu_{\text{B}}$  ( $25^\circ$ ,  $d_6$ -DMSO) similar to other five-coordinate Ni(II) species having high-spin,  $S = 1$  ground-states.<sup>31–37</sup> The UV-visible absorption spectra for  $[\text{Ni}(\text{L}^{\text{iPr}})]^-$ ,  $[\text{Ni}(\text{L}^{\text{tBu}})]^-$ , and  $[\text{Ni}(\text{L}^{\text{Ph}})(\text{CH}_3\text{CN})]^-$  were recorded at room temperature as  $N,N$ -dimethylformamide (DMF) solutions. The four-coordinate complexes,  $[\text{Ni}(\text{L}^{\text{iPr}})]^-$  and  $[\text{Ni}(\text{L}^{\text{tBu}})]^-$ , exhibit similar spectra with  $\lambda_{\text{max}}$  values at 525 and 520 nm, respectively. The five-coordinate species,  $[\text{Ni}(\text{L}^{\text{Ph}})(\text{CH}_3\text{CN})]^-$ , exhibits a broad absorbance centred at 707 nm. A similar broad absorbance (694 nm) has been observed and its transitions assigned ( $^3E'(F) \rightarrow ^3A_1'(F)$ ,  $^3A_2'(F)$ ) for a high-spin trigonal bipyramidal Ni(II) complex containing an  $\text{N}_2\text{O}_3$  donor set.<sup>32,38</sup>

### Cyanide coordination

The differences in coordination number and environment exhibited by  $[\text{Ni}(\text{L}^{\text{iPr}})]^-$ ,  $[\text{Ni}(\text{L}^{\text{tBu}})]^-$ , and  $[\text{Ni}(\text{L}^{\text{Ph}})(\text{CH}_3\text{CN})]^-$  prompted us to explore the ability of these complexes to coordinate exogenous ligands. Specifically, we sought to explore the ability of these complexes to bind cyanide because it is a small, linear donor. The orange  $[\text{Ni}(\text{L}^{\text{iPr}})]^-$  complex reacts readily with one equivalent of tetraethylammonium cyanide ( $[\text{Et}_4\text{N}]\text{CN}$ ) to produce a green solution. We formulate the nickel-containing product of this reaction to be  $[\text{Ni}(\text{L}^{\text{iPr}})(\text{CN})]^{2-}$  by spectroscopic match to an authentic sample prepared directly from the protio ligand in a one-pot procedure (see Experimental section for details).

The dianionic cyanide complex,  $[\text{Ni}(\text{L}^{\text{iPr}})(\text{CN})]^{2-}$ , exhibits a cyanide stretch in the IR spectrum at  $2112\text{ cm}^{-1}$  consistent with a terminally bound cyanide ligand.<sup>39</sup> This complex is paramagnetic and exhibits a  $\mu_{\text{eff}}$  value of 3.25  $\mu_{\text{B}}$  ( $25^\circ$ ,  $d_6$ -DMSO) indicating a high-spin,  $S = 1$  system (*vide supra*). This species can be recrystallized by the slow diffusion of diethyl ether into a concentrated DMF solution of the complex to afford X-ray quality crystals. Results of the single crystal X-ray diffraction studies carried out on  $[\text{Et}_4\text{N}]_2[\text{Ni}(\text{L}^{\text{iPr}})(\text{CN})]$  are shown in Fig. 2. Crystals of  $[\text{Et}_4\text{N}]_2[\text{Ni}(\text{L}^{\text{iPr}})(\text{CN})]$  form in a  $P2_1/n$  space group with  $Z = 8$ . There are two crystallographically independent and geometrically dissimilar  $[\text{Ni}(\text{L}^{\text{iPr}})(\text{CN})]^{2-}$  units within the asymmetric unit cell. Both nickel centres are five-coordinate and contain the same donor atoms within their primary coordination sphere. Each Ni(II) ion is coordinated by three  $N$ -amidate and one tertiary amine donor of the chelating ligand and a terminal cyanide ligand. In one of the anions,  $[\text{Ni}1(\text{L}^{\text{iPr}})(\text{CN})]^{2-}$  (Fig. 2A), the nickel centre displays a distorted square pyramidal geometry. The other nickel centre,  $[\text{Ni}2(\text{L}^{\text{iPr}})(\text{CN})]^{2-}$  (Fig. 2B), exhibits a distorted trigonal bipyramidal coordination geometry. For five-coordinate species, the degree of distortion between idealized trigonal bipyramidal

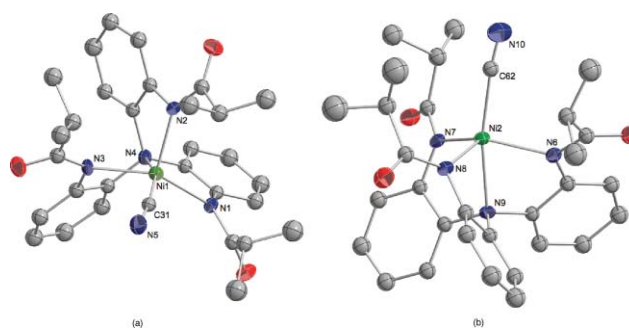


**Fig. 2** Thermal ellipsoid diagrams of the two independent anions found in the asymmetric unit of  $[\text{Et}_4\text{N}]_2[\text{Ni}(\text{L}^{\text{iPr}})(\text{CN})]$ ; (A)  $[\text{Ni}1(\text{L}^{\text{iPr}})(\text{CN})]^{2-}$  and (B)  $[\text{Ni}2(\text{L}^{\text{iPr}})(\text{CN})]^{2-}$  drawn at 35% probability. Hydrogen atoms and counter cations have been removed for clarity. Selected bond lengths ( $\text{\AA}$ ) and angles ( $^\circ$ ) for (A) Ni1–N1 2.091(5), Ni1–N2 2.027(4), Ni1–N3 2.083(4), Ni1–N4 2.122(5), Ni1–C31 2.018(6), N4–Ni1–C31 158.9(2), N3–Ni1–N1 143.25, N2–Ni1–C31 116.7(2), N4–Ni1–N3 76.29(18), N4–Ni1–N1 80.77(18), Ni1–C31–N5 167.2(6); and (B): Ni2–N9 2.139(4), Ni2–N8 2.023(5), Ni2–N7 2.101(5), Ni2–N6 2.089(5), Ni2–C62 2.019(7), N9–Ni2–C62 169.0(2), N6–Ni2–N7 133.76(17), N6–Ni2–N8 106.21(18), N7–Ni2–N8 106.65(18), Ni2–C62–N10 173.6(6).

and square pyramidal geometries can be quantified by using the  $\tau_5$  parameter defined by Addison and Reedijk.<sup>40</sup> The value of  $\tau_5$  varies between 0.0 (for idealized square pyramidal geometry) and 1.0 (for idealized trigonal bipyramidal geometry). Applying this structural parameter to  $[\text{Ni}1(\text{L}^{\text{iPr}})(\text{CN})]^{2-}$  and  $[\text{Ni}2(\text{L}^{\text{iPr}})(\text{CN})]^{2-}$  gives rise to  $\tau_5$  values of 0.26 and 0.59, respectively, illustrating their intermediate geometries. Co-crystallization of geometrical<sup>40–46</sup> or polytopal isomers<sup>46–48</sup> within the same unit cell has been observed for other transition metal systems. Co-crystallization of these species is rare, however, because compounds with different molecular structures typically possess different crystallization kinetics and crystal lattice packing energies.<sup>49</sup> These structural data suggest that the two geometries observed for  $[\text{Ni}(\text{L}^{\text{iPr}})(\text{CN})]^{2-}$  in the solid-state are very similar in energy and that, in solution, a distribution of these geometries must exist. In solution,  $[\text{Ni}(\text{L}^{\text{iPr}})(\text{CN})]^{2-}$  displays a single, quasi-reversible electrochemical event ( $50\text{ mV s}^{-1}$ ) in its cyclic voltammogram centred at  $-251\text{ mV}$  (Fig. S1 in ESI†). We tentatively assign this process to the  $\text{Ni}^{\text{III/II}}$  couple.

When the  $[\text{Ni}(\text{L}^{\text{tBu}})]^-$  complex is treated with cyanide, a slight colour change from orange to red-orange is observed. This reaction, however, does not give rise to a single, well-defined product in solution. Both solution-state IR and  $^1\text{H}$  NMR spectroscopy indicate that cyanide does interact to some extent with the nickel centre. For example, in the solution-state FT-IR spectrum ( $\text{CH}_3\text{CN}$ ) a major  $\nu_{\text{CN}}$  stretching band appears at  $2109\text{ cm}^{-1}$ , suggesting coordination of the cyanide ligand in a terminal fashion,<sup>39</sup> similar to what is observed for the isolated  $[\text{Ni}(\text{L}^{\text{iPr}})(\text{CN})]^{2-}$  species (*vide supra*). However, several lower intensity, higher frequency bands also appear ( $2150\text{ cm}^{-1}$  and  $2186\text{ cm}^{-1}$ ) that cannot be definitely assigned. The  $^1\text{H}$  NMR spectrum ( $\text{CD}_3\text{CN}$ ) also reveals the presence of at least two major species in solution. One of the species is paramagnetic and exhibits a spectrum nearly identical to the  $[\text{Ni}(\text{L}^{\text{tBu}})]^-$  starting material. The second species is diamagnetic and exhibits three distinct  $^1\text{Bu}$  resonances. These data are consistent with the existence of a solution-state equilibrium between a diamagnetic, square planar complex and a paramagnetic species. We propose that cyanide

coordination to the nickel centre in  $[\text{Ni}(\text{L}^{\text{bu}})]^-$  may cause one of the coordinated ligand arms to dissociate to afford a square planar species. Similar solution-state equilibria have recently been observed for nickel complexes supported by scorpionate ligands.<sup>50</sup> The  $[\text{Ni}(\text{L}^{\text{ph}})(\text{CH}_3\text{CN})]^-$  complex also reacts with cyanide to produce a complex reaction mixture that contains both paramagnetic and diamagnetic products. This result was somewhat surprising as the solid-state data obtained for  $[\text{Ni}(\text{L}^{\text{ph}})(\text{CH}_3\text{CN})]^-$  clearly demonstrates the ability of this ligand to support five-coordinate Ni(II) species. One possible explanation for this result is that the association constant for acetonitrile binding to  $[\text{Ni}(\text{L}^{\text{ph}})]^-$  is greater than the association constant for cyanide. Further studies probing these observations are underway in our laboratories.

### Solid-state magnetic properties of selected mononuclear Ni complexes

The unusual ligand field environment for Ni(II) ions provided by the tris-amidate ligand architecture may influence magnetic anisotropy parameters, which are of interest in the field of molecular magnetism.<sup>51,52</sup> Thus, solid-state magnetic susceptibility studies were undertaken for  $\text{Ph}_4\text{P}[\text{Ni}(\text{L}^{\text{ipr}})]$  and  $[\text{Et}_4\text{N}]_2[\text{Ni}(\text{L}^{\text{ipr}})(\text{CN})]$ . A plot of the temperature dependence of  $\chi_{\text{M}}T$  for  $[\text{Et}_4\text{N}]_2[\text{Ni}(\text{L}^{\text{ipr}})(\text{CN})]$  (obtained at 0.1 T) appears in Fig. 3. Here, the  $\chi_{\text{M}}T$  value of 1.46 emu K mol<sup>-1</sup> at 300 K is significantly larger than that expected for a mononuclear Ni(II) complex with  $S = 1$  and  $g = 2.00$  (1.00 emu K mol<sup>-1</sup>). The product decreases gradually to 1.32 emu K mol<sup>-1</sup> at 50 K, followed by a steep drop to 0.56 emu K mol<sup>-1</sup> at 2 K. Qualitatively similar data are obtained for  $\text{Ph}_4\text{P}[\text{Ni}(\text{L}^{\text{ipr}})]$  (ESI Fig. S2†).

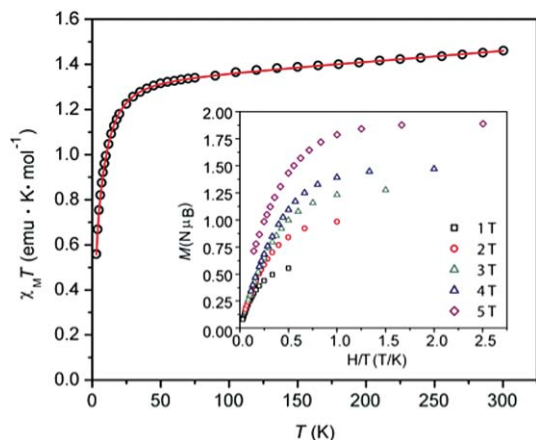


**Fig. 3** Temperature dependence of magnetic susceptibility for  $[\text{Et}_4\text{N}]_2[\text{Ni}(\text{L}^{\text{ipr}})(\text{CN})]$  obtained at a measuring field of 0.1 T. Best fits to the data (red line) give  $g = 2.295$ ,  $D = -23.03 \text{ cm}^{-1}$ ,  $E = -2.60 \text{ cm}^{-1}$ , TIP =  $475 \times 10^{-6} \text{ emu mol}^{-1}$ , and relative error  $f = 0.005$ . Inset: Magnetization of  $[\text{Et}_4\text{N}]_2[\text{Ni}(\text{L}^{\text{ipr}})(\text{CN})]$  as a function of reduced magnetic field.

Fitting the susceptibility data to a magnetic model, we first considered the most likely scenario, in which unpaired spin localizes on the Ni center (*i.e.* Ni(II),  $S = 1$ ). For  $\text{Ph}_4\text{P}[\text{Ni}(\text{L}^{\text{ipr}})]$ , the best fit affords  $g = 2.35$ ,  $D = -19.44 \text{ cm}^{-1}$ ,  $E = -1.46 \text{ cm}^{-1}$ , temperature independent paramagnetism (TIP) =  $808 \times 10^{-6} \text{ emu mol}^{-1}$ , and relative error  $f = 0.018$ . Similarly, the best fit for  $[\text{Et}_4\text{N}]_2[\text{Ni}(\text{L}^{\text{ipr}})(\text{CN})]$  gives  $g = 2.295$ ,  $D = -23.03 \text{ cm}^{-1}$ ,  $E = -2.60 \text{ cm}^{-1}$ , TIP =  $475 \times 10^{-6} \text{ emu mol}^{-1}$ , and relative error  $f = 0.005$ . In both cases, the

fitted  $|D|$  and TIP values are significantly larger than might be expected. The former may be due to weak intermolecular interactions being incorporated into the phenomenological  $D$  parameter (although no obvious exchange pathways are present in the crystal structures); the latter may be indicative of low lying excited spin states, and similar values have been reported for a Ni(II) porphyrin complex.<sup>53</sup> Nevertheless, we considered two other alternatives. The potential coupling of a Ni(I) center ( $S = \frac{1}{2}$ ) with a radical dianionic ligand did not result in any reasonable fits to the data. Alternatively, antiferromagnetic coupling of a high spin Ni(III) center ( $S = 3/2$ ) with a radical tetraanionic ligand ( $S = \frac{1}{2}$ ) afforded large intramolecular exchange coupling ( $J \sim -5000 \text{ cm}^{-1}$ ) and a reasonable  $g_{\text{Ni}}$  of  $\sim 2.3$ , but only when the radical  $g$  was fixed at 2.00; even then, the fits were inferior to the original scenario.

To examine magnetic anisotropy in more detail, we collected magnetization data at various fields between 2 and 35 K (Fig. 3, inset). The data collected at different fields do not overlay each other, and deviate significantly from the Brillouin function expected for  $S = 1$ , indicating significant zero-field splitting. However, modeling the data with ANISOFIT<sup>54</sup> does not afford satisfactory fits, even when we restrict fitting to the lowest temperatures ( $< 14 \text{ K}$ ). The lack of agreement is likely due to the presence of low lying excited spin states; unfortunately ANISOFIT requires well isolated ground spin states to give the best fits. We conclude that an  $S = 1$  Ni(II) ion with significant (but complicated) zero-field splitting is operative in these compounds.

### Formation of a heterobimetallic complex

The ability of  $[\text{Ni}(\text{L}^{\text{ipr}})]^-$  to irreversibly bind cyanide in solution is unique for this series of complexes. We next sought to investigate whether  $[\text{Ni}(\text{L}^{\text{ipr}})(\text{CN})]^{2-}$  could be used to form heterobimetallic complexes. Our motivation for this study is based upon the widespread utility of terminal cyanide complexes in the assembly of molecular, cyanide-bridged clusters *via* the “building block approach.”<sup>51,52,55–57</sup> Cyanide complexes with terminal cyanide ligands or open binding sites are often used as capping or blocking groups in the construction of these species. Thus, the reaction of green  $[\text{Ni}(\text{L}^{\text{ipr}})(\text{CN})]^{2-}$  with a four-coordinate, trigonal pyramidal Co(II) complex of the same ligand,  $[\text{Co}(\text{L}^{\text{ipr}})]^-$ ,<sup>26</sup> immediately produces a reddish-violet solution. The product of this reaction is isolated as a reddish-purple solid in good yield (83%). FT-IR studies suggest a bridging coordination mode of the cyanide ligand, as the product exhibits a single  $\nu_{\text{CN}}$  (KBr) stretch at  $2126 \text{ cm}^{-1}$ . The increase in cyanide stretching frequency observed for the product compared to the mononuclear nickel cyanide precursor, is consistent with the formation of a cyanide-bridged species.<sup>55</sup>

Crystals of X-ray quality were grown by the diffusion of diethyl ether into a concentrated DMF solution of the product. The molecular structure of the heterobimetallic complex,  $[\text{Et}_4\text{N}]_3[\text{CoNi}(\text{L}^{\text{ipr}})_2(\mu_2\text{-CN})]$  is shown in Fig. 4. The trianionic complex crystallizes in a rhombohedral space group ( $R\bar{3}$ ) and adopts 3-fold symmetry. The crystals contained poorly resolved solvent peaks and there was some disorder in the pendant arms of the tetraethylammonium cations. Nevertheless, the  $[\text{CoNi}(\text{L}^{\text{ipr}})_2(\mu_2\text{-CN})]^{3-}$  unit is well-resolved. To be confident that the correct molecular geometry had been assigned, the nickel and cobalt atoms were exchanged as well as the carbon and

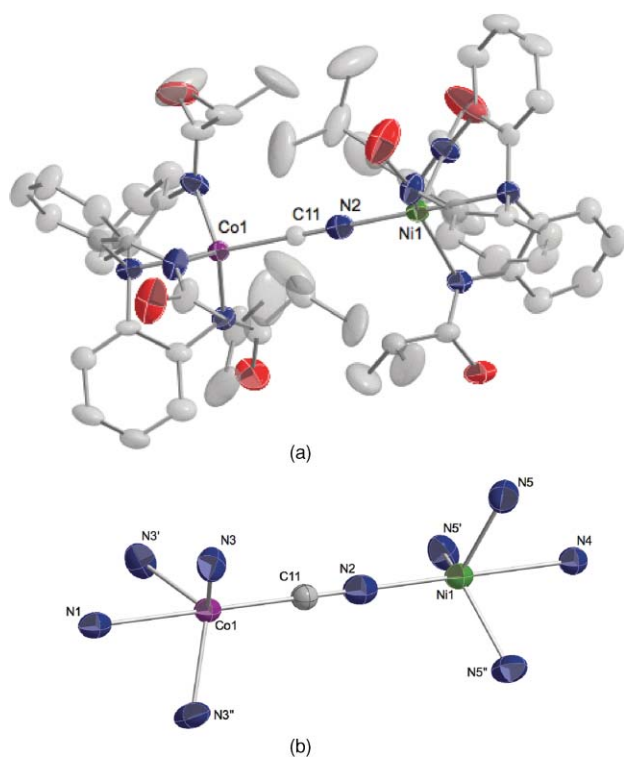


**Fig. 4** Thermal ellipsoid diagrams (35%) of (A)  $[\text{CoNi}(\text{L}^{\text{iPr}})_2(\mu_2\text{-CN})]^{2-}$  and (B) the core structure of  $[\text{CoNi}(\text{L}^{\text{iPr}})_2(\mu_2\text{-CN})]^{2-}$ . Hydrogen atoms and counter ions have been removed for clarity. Selected bond lengths ( $\text{\AA}$ ) and angles ( $^\circ$ ): Co–N1 2.354(9); Co–N3 2.035(4); Co–C11 2.029(13); Ni–N4 2.390(9); Ni–N5 2.030(4); Ni–N2 2.063(12); C11–N2 1.167(7); N1–Co–C11 180.00(1); C11–N2–Ni 180.00(1); C11–Co–N3 105.59(11); N3–Co–N3' 113.06(9); N3–Co–N1 74.41(11); N2–Ni–N5 105.86(11); N5–Co–N5' 112.83(9); N5–Ni–N4 74.14(11).

nitrogen atoms of the bridging cyanide ligand and their final positions verified after least squares analysis by critical evaluation of their respective atomic displacement parameters. Note that the orientation of the cyanide bridging ligand in  $[\text{CoNi}(\text{L}^{\text{iPr}})_2(\mu_2\text{-CN})]^{2-}$  is different from that observed in the  $[\text{Et}_4\text{N}]_2[\text{Ni}(\text{L}^{\text{iPr}})(\text{CN})]$  precursor, *i.e.*, the cyanide ligand is coordinated to the nickel centre *via* the nitrogen atom. This type of cyanide flipping or linkage isomerism has been observed in the formation of other bridged cyanide clusters.<sup>58</sup>

The Ni(II) and Co(II) centres both display distorted trigonal bipyramidal coordination geometries with  $\text{M}(\text{II})\text{-N}_{\text{amidate}}$  bond length similar to those observed in the mononuclear complexes. Each metal centre displays relatively long ( $< 2.3 \text{ \AA}$ )  $\text{M}(\text{II})\text{-N}_{\text{amine}}$  bond lengths.<sup>59</sup> Long  $\text{M}(\text{II})\text{-N}_{\text{tertiary amine}}$  bond distances have been observed in other dinuclear Ni(II)<sup>60–64</sup> and Co(II)<sup>65–67</sup> complexes supported by sterically demanding ligands. The  $\text{M}(\text{II})\text{-N}_{\text{apical}}$  elongation observed in  $[\text{CoNi}(\text{L}^{\text{iPr}})_2(\mu_2\text{-CN})]^{2-}$  is likely to be due to the geometric distortions that occur upon formation of the bimetallic complex. Specifically, the two  $[\text{L}^{\text{iPr}}]^{3-}$  ligands which cap the Co(II) and Ni(II) centres are positioned so that the isopropyl substituents are interlocked about the bridging cyanide ligand, forcing a completely linear N1–Co–C $\equiv$ N–Ni–N4 arrangement of atoms within the molecule. In addition, both the Co(II) and Ni(II) centres are distorted  $\sim 0.55 \text{ \AA}$  away from the trigonal planes formed by the *N*-amidate donors of the  $[\text{L}^{\text{iPr}}]^{3-}$  ligands

toward the bridging cyanide. This type of co-linear arrangement of atoms within multimetallic assemblies has been previously observed in binuclear Cu(II) cryptates<sup>68,69</sup> and in Co(II) cyanide clusters assembled with capping ligands.<sup>70</sup> These results suggest that transition metal complexes supported by  $[\text{L}^{\text{R}}]^{3-}$  type ligands may be useful as capping species in the assembly of larger molecular clusters.<sup>71</sup>

#### Magnetism of $[\text{Et}_4\text{N}]_3[\text{CoNi}(\text{L}^{\text{iPr}})_2(\mu_2\text{-CN})]$

A plot of the temperature dependence of  $\chi_{\text{M}}T$  (obtained at 0.1 T) appears in Fig. 5. The  $\chi_{\text{M}}T$  value at 300 K is  $5.07 \text{ emu K mol}^{-1}$ , which again is significantly larger than expected for non-interacting  $S = 1$  Ni(II) and  $S = 3/2$  Co(II) spin centres ( $2.875 \text{ emu K mol}^{-1}$ ). The product decreases linearly (due to Co(II) orbital moment and/or TIP) to  $3.59 \text{ emu K mol}^{-1}$  at 70 K. At lower temperatures, the susceptibility drops off more rapidly to  $0.86 \text{ emu K mol}^{-1}$  at 3 K. Using JulX,<sup>72</sup> and assuming no zero-field splitting, the best fit to the data indicates weak antiferromagnetic coupling between the Co(II) and Ni(II) ions ( $J = -2.04 \text{ cm}^{-1}$ ). This is consistent with expected weak superexchange (through cyanide  $\pi^*$  orbitals) between the singly-occupied molecular orbitals of the constituent ions, which for Ni(II) and Co(II) ions should have the same symmetries.<sup>51,73</sup> A large TIP value is observed, consistent both with the Ni-CN complex  $[\text{Et}_4\text{N}]_2[\text{Ni}(\text{L}^{\text{iPr}})(\text{CN})]$  as well as distortion of the local coordination sphere around the Co(II), which is known to give large TIP and Zeeman contributions to the susceptibility.<sup>74</sup>

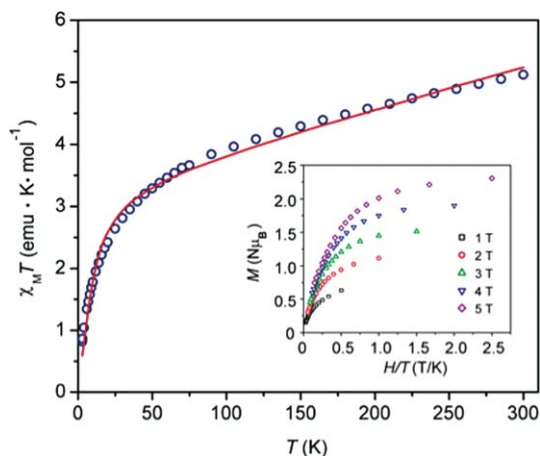


**Fig. 5** Temperature dependence of magnetic susceptibility for  $[\text{Et}_4\text{N}]_3[\text{CoNi}(\text{L}^{\text{iPr}})_2(\mu_2\text{-CN})]$  obtained at a measuring field of 0.1 T. Assuming no zero-field splitting ( $D$  and  $E$  fixed at 0), best fits to the data (red line) give  $J = 2.04 \text{ cm}^{-1}$ ,  $g = 2.15$ ,  $\text{TIP} = 6600 \times 10^{-6} \text{ emu mol}^{-1}$ , and relative error  $f = 0.11$ . Inset: Magnetization of  $[\text{Et}_4\text{N}]_3[\text{CoNi}(\text{L}^{\text{iPr}})_2(\mu_2\text{-CN})]$  as a function of reduced magnetic field.

As with the mononuclear complexes, magnetization data (inset, Fig. 4) clearly show significant magnetic anisotropy; however, this data does not yield reasonable fits using ANISOFIT. In addition to the issues described above for the mononuclear Ni(II) precursor, it has been shown that fitting magnetization data with Co(II) complexes can be difficult due to the mixing of low-lying excited states into the ground state,<sup>75</sup> as well as the presence of Zeeman effects. Evidence for the latter behavior is shown in the ESI, Fig. S3,<sup>†</sup> where the susceptibility data at higher fields tracks

under those obtained at lower fields.<sup>76</sup> If  $D$  is included in the fits to the susceptibility data (ESI, Fig. S4 and S5†), the quality improves somewhat when the parameter is allowed to refine freely, affording  $D = 20 \text{ cm}^{-1}$ . As  $|D|$  values for Co(II) complexes are typically  $1 \text{ cm}^{-1}$  to  $5 \text{ cm}^{-1}$ ,<sup>77</sup> this large value would appear to trace back to the presence of Ni(II), similar to the mononuclear species. In spite of the rather weak coupling, the apparently large values of magnetic anisotropy merit further study. Efforts along these lines are underway.

## Conclusions

In summary, nickel(II) complexes supported by a family of chelating tris(amidate) ligands,  $[\text{N}(o\text{-PhNC(O)R})_3]^{3-}$  ( $[\text{L}^{\text{R}}]^{3-}$  where  $\text{R} = \text{}^i\text{Pr}$ ,  $\text{}^t\text{Bu}$ , and  $\text{Ph}$ ), have been prepared and characterized. The nickel centres in  $[\text{Ni}(\text{L}^{\text{iPr}})]^-$  and  $[\text{Ni}(\text{L}^{\text{tBu}})]^-$  exhibit similar coordination geometries but different primary coordination spheres. In  $[\text{Ni}(\text{L}^{\text{iPr}})]^-$ , the four-coordinate Ni(II) ion is ligated by a tertiary amine and three  $N$ -amidate donors of the ligand. In contrast, the nickel centre in  $[\text{Ni}(\text{L}^{\text{tBu}})]^-$  is coordinated by a tertiary amine, one  $O$ -amidate donor, and two  $N$ -amidate donors of the ligand. The phenyl ligand derivative,  $[\text{L}^{\text{Ph}}]^{3-}$ , stabilizes nickel(II) as a five-coordinate solvento adduct,  $[\text{Ni}(\text{L}^{\text{Ph}})(\text{CH}_3\text{CN})]^-$ . We propose that the amidate substituents are regulating the coordination motifs observed in this series of complexes. The ability of these nickel complexes to bind cyanide has also been investigated. Only one of the complexes,  $[\text{Ni}(\text{L}^{\text{iPr}})]^-$ , irreversibly binds cyanide to form an isolable cyanide complex,  $[\text{Ni}(\text{L}^{\text{iPr}})(\text{CN})]^{2-}$ .  $[\text{Ni}(\text{L}^{\text{iPr}})(\text{CN})]^{2-}$  is capable of adopting either trigonal bipyramidal or square pyramidal geometries in the solid-state and can be used to assemble a cyanide-bridged, heterobimetallic complex. The unusual ligand fields presented by this family of ligands engender interesting, if complicated, magnetic behaviour in the Ni(II) complexes studied, and merit more in-depth investigation. Overall, these studies demonstrate that these chelating tris(amidate) ligands offer highly tuneable and versatile scaffolds for Ni(II).

## Experimental

### General considerations

All manipulations were carried out using standard Schlenk techniques or conducted in an MBraun Labmaster 130 drybox under a dinitrogen atmosphere. All reagents used were purchased from commercial vendors and used as received unless otherwise stated. Anhydrous solvents were purchased from Sigma-Aldrich and further purified by sparging with Ar gas followed by passage through activated alumina columns. Anhydrous  $\text{NiBr}_2$  was purchased from Strem Chemical, Inc. Deuterated solvents were purchased from Sigma Aldrich or Cambridge Isotope Laboratories, Inc. and degassed and dried according to standard procedures prior to use. Elemental analyses were performed by Columbia Analytical Services, Tucson, AZ or Atlantic Microlab, Inc., Norcross, GA.  $^1\text{H}$  and  $^{13}\text{C}$  NMR spectra were recorded on a Varian Mercury 300 MHz spectrometer at ambient temperature. Chemical shifts were referenced to residual solvent peaks. Infrared spectra were recorded as KBr pellets on a Varian Scimitar 800 Series FT-IR spectrophotometer. UV-Visible absorption spectra were recorded on a Cary 50 spectrophotometer using 1.0 cm quartz cuvettes. All

samples were prepared under an  $\text{N}_2$  atmosphere. Solution state magnetic moments were measured using the Evans method.<sup>29,30</sup> Mass spectra were recorded in the Mass Spectrometry Center at Emory University on a JEOL JMS-SX102/SX102A/E mass spectrometer. Cyclic voltammetric experiments were carried out using a CH Instruments (Austin, TX) Model 660C potentiostat. All electrochemistry experiments were conducted in DMF with 0.20 M tetrabutylammonium hexafluorophosphate as the supporting electrolyte. Electrochemical experiments were conducted using a three-component cell consisting of a Pt auxiliary electrode, a non-aqueous reference electrode ( $\text{Ag}/\text{AgNO}_3$ ), and a glassy carbon working electrode. All electrochemical measurements are referenced and reported *versus* the ferrocene/ferrocenium couple.

$\text{PPh}_4\text{CN}$  was prepared using a literature procedure.<sup>78</sup> The ligand precursor,  $\text{N}(o\text{-PhNH}_2)_3$ ,<sup>26</sup> and the ligands  $\text{H}_3\text{L}^{\text{iPr}}$ <sup>26</sup> and  $\text{H}_3\text{L}^{\text{tBu}}$ <sup>27</sup> were synthesized using previously published procedures.

### 2,2',2''-trisphenylamidotriphenylamine, $\text{H}_3\text{L}^{\text{Ph}}$

A suspension of  $\text{N}(o\text{-PhNH}_2)_3$  (2.01 g, 6.93 mmol) in dichloromethane (DCM, 40 mL) was lowered to  $0^\circ\text{C}$  under an atmosphere of  $\text{N}_2$ . Triethylamine (3.09 mL, 22.2 mmol) was then added, followed by benzoyl chloride (2.57 mL, 22.2 mmol). The mixture was stirred for 90 min and was allowed to warm to room temperature. The reaction mixture was washed with aqueous HCl (0.1 M, 100 mL), dried over magnesium sulfate, and concentrated *in vacuo*; yielding a green oil. Crystals of the product were obtained by layering petroleum ether onto a concentrated DCM solution and cooling to  $-40^\circ\text{C}$  (3.53 g, 85%).  $^1\text{H}$  NMR ( $\delta$ ,  $\text{CD}_3\text{CN}$ , 300 MHz): 9.16 (s, 3H, NH), 7.66 (t, 3H,  $J = 4.2$  Hz, ArH), 7.45 (t, 3H,  $J = 7.5$  Hz, ArH), 7.40 (d, 6H,  $J = 7.2$  Hz, ArH), 7.30 (t, 6H,  $J = 7.5$  Hz, ArH), 7.10 (t, 6H,  $J = 3.9$  Hz, ArH), 6.90 (m, 3H, ArH).  $^{13}\text{C}$  NMR ( $\delta$ ,  $\text{CD}_3\text{CN}$ , 300 MHz): 166.55, 139.46, 135.43, 133.09, 133.03, 129.50, 128.52, 127.45, 126.69, 126.13, 125.76. HRESI-MS:  $\text{C}_{39}\text{H}_{31}\text{O}_3\text{N}_4$   $m/z$  Calcd. 603.23907 Found 603.23914  $[\text{M}+1]^+$ . FTIR (KBr,  $\text{cm}^{-1}$ ):  $\nu(\text{NH})$  3273,  $\nu(\text{CO})$  1655.

### $[\text{Ph}_4\text{P}][\text{Ni}(\text{L}^{\text{iPr}})]$

To a solution of  $\text{H}_3\text{L}^{\text{iPr}}$  ( $\text{H}_3\text{L}^{\text{iPr}} = \text{N}(o\text{-PhNHC}(O)^i\text{Pr})_3$ ) (117 mg, 0.23 mmol) in dry DMF (3 mL) was added solid potassium hydride (31 mg, 0.77 mmol). When hydrogen gas evolution ceased ( $\sim 40$  min),  $\text{NiBr}_2$  (51 mg, 0.23 mmol) was added as a solid and the reaction stirred for four hours. Tetraphenylphosphonium bromide (98 mg, 0.23 mmol) was added to the deep orange solution as a solid. After stirring for 1 h, the solution was concentrated *in vacuo* to yield an orange solid. The resulting orange solid was then dissolved in  $\text{CH}_3\text{CN}$  and filtered through a sintered glass frit to remove KBr. The filtrate was concentrated under reduced pressure and the product isolated as an orange solid. X-ray quality crystals were obtained by the slow diffusion of diethyl ether into a DMF solution of the complex to give orange crystals (109 mg, 68%).  $^1\text{H}$  NMR ( $\delta$ ,  $\text{CD}_3\text{CN}$ , 300 MHz): 21.38 (br), 19.98 (sh), 7.64 m, 16H and 7.86 t, 4H  $-\text{PPh}_4^+$ , 2.16 (br). FTIR (KBr,  $\text{cm}^{-1}$ ):  $\nu$ : 3059, 3020, 2959, 2926, 2866, 1677 ( $\text{CO}_{\text{DMF}}$ ), 1604 (CO), 1578, 1476, 1440, 1386, 1295, 1276, 1207, 1108, 1040, 967, 767, 724, 690, 527.  $\mu_{\text{eff}} = 3.03 \mu_{\text{B}}$  (Evans Method,  $(\text{CD}_3)_2\text{SO}$ , 298 K).  $\lambda_{\text{max}}(\epsilon, \text{M}^{-1} \text{cm}^{-1})$  (DMF): 401(794) 525 (69) Anal. Calcd (found)

for  $\text{Ph}_4\text{P}[\text{NiL}^{\text{iPr}}]\cdot 2\text{DMF}$ : C, 69.17 (69.35); H, 6.48 (6.35); N, 8.07 (8.15).

### $[\text{Ph}_4\text{P}][\text{Ni}(\text{L}^{\text{Ph}})(\text{MeCN})]$

To a stirred solution of  $\text{H}_3\text{L}^{\text{Ph}}$  ( $\text{H}_3\text{L}^{\text{Ph}} = \text{N}(o\text{-PhNHC}(O)\text{Ph})_3$ ) (361 mg, 0.60 mmol) in DMF (5 mL) was added KH (79 mg, 1.98 mmol) as a solid. When  $\text{H}_2$  evolution ceased (~30 min),  $\text{NiBr}_2$  (131 mg, 0.60 mmol) was added as a solid. The pale yellow solution turned orange as the metal salt dissolved over a period of four hours. Tetraphenylphosphonium bromide (251 mg, 0.60 mmol) was added as a solid. After 30 min of stirring, solvent was removed under reduced pressure. The resulting yellow oil was dissolved in acetonitrile (40 mL) and filtered to remove KBr. The filtrate was concentrated under reduced pressure, and the resulting yellow-green solid was recrystallized from acetonitrile (409 mg, 66%). X-ray quality crystals were obtained by vapor diffusion of diethyl ether into a concentrated acetonitrile solution of the complex.  $^1\text{H}$  NMR ( $\delta$ ,  $\text{CD}_3\text{CN}$ , 300 MHz): 48.36 (br), 21.14 (sh), 12.41 (sh), 9.18 (sh), 7.73 t, 4H and 7.53 m, 16H  $-\text{PPh}_4^+$ , -8.63 (sh), -29.87 (br). FTIR (KBr,  $\text{cm}^{-1}$ )  $\nu$ : 3056, 3021, 2927, 2247 ( $\text{CH}_3\text{CN}$ ), 1596 (CO), 1584, 1552, 1473, 1442, 1357, 1109, 1041, 997, 914, 754, 723, 690, 527.  $\mu_{\text{eff}} = 3.27 \mu_{\text{B}}$  (Evans Method,  $\text{DMSO}-d_6$ , 298 K).  $\lambda_{\text{max}}(e, \text{M}^{-1}\text{cm}^{-1})$  (DMF): 707(16). Sample for elemental analysis was prepared by the diffusion of diethyl ether into a concentrated DMF solution of the complex. The presence of one DMF solvent per complex was confirmed by  $^1\text{H}$  NMR and integrated *versus* the  $\text{PPh}_4^+$  counterion. Anal. Calcd (found) for  $\text{Ph}_4\text{P}[\text{NiN}(o\text{-PhNC}(O)\text{Ph})_3(\text{MeCN})]\cdot\text{DMF}$ : C, 73.45 (73.32); H, 5.17 (5.01); N, 7.56 (7.67).

### $[\text{Ph}_4\text{P}][\text{Ni}(\text{L}^{\text{iBu}})]$

To a solution of  $\text{H}_3\text{L}^{\text{iBu}}$  ( $\text{H}_3\text{L}^{\text{iBu}} = \text{N}(o\text{-PhNHC}(O)^{\text{iBu}})_3$ ) (426 mg, 0.79 mmol) in dry DMF (50 mL) was added solid potassium hydride (104 mg, 2.59 mmol). A colorless precipitate formed. When all of the solid dissolved,  $\text{NiBr}_2$  (172 mg, 0.79 mmol) was added as a solid and the reaction stirred for four hours. Tetraphenylphosphonium bromide (329 mg, 0.79 mmol) was added to the deep orange solution as a solid. After stirring for 1 h, the solution was concentrated *in vacuo*. The resultant orange powder was dissolved in MeCN and filtered to yield the final product as an orange solid. X-ray quality crystals could be obtained by the slow diffusion of diethyl ether into DMF to give orange crystals (271 mg, 37%).  $^1\text{H}$  NMR ( $\delta$ ,  $\text{CD}_3\text{CN}$ , 300 MHz): 53.99 (br), 39.64 (br), 31.00 (br), 25.07 (br), 22.44 (sh), 21.93 (br), 21.27 (br), 17.15 (sh), 14.32 (br), 13.70 (sh), 9.89 (sh), (7.90 t, 4H and 7.70 m, 16H  $-\text{PPh}_4^+$ ), 0.17 (br), -1.51 (sh), -3.1 (br), -5.09 (sh), -18.8 (br), -19.4 (sh). FTIR (KBr,  $\text{cm}^{-1}$ )  $\nu$ : 3057, 2949, 2919, 2861, 1597 (CO), 1557, 1475, 1439, 1387, 1328, 1244, 1195, 1172, 1108, 1045, 997, 951, 756, 724, 691, 528, 483.  $\mu_{\text{eff}} = 3.37 \mu_{\text{B}}$  (Evans Method,  $\text{CD}_3\text{CN}$ , 298 K).  $\lambda_{\text{max}}(e, \text{M}^{-1}\text{cm}^{-1})$  (DMF): 520 (119). Anal. Calcd (found) for  $\text{Ph}_4\text{P}[\text{NiN}(o\text{-PhNC}(O)^{\text{iBu}})_3]\cdot\text{DMF}$ : C, 71.29 (70.88); H, 6.58 (6.61); N, 6.93 (6.80).

### $[\text{Et}_4\text{N}]_2[\text{Ni}(\text{L}^{\text{iPr}})(\text{CN})]$

To a solution of  $\text{H}_3\text{L}^{\text{iPr}}$  (68 mg, 0.14 mmol) in dry DMF (3 mL) was added solid potassium hydride (18 mg, 0.45 mmol). When the reaction mixture was completely homogeneous,  $\text{NiBr}_2$  (30 mg,

0.14 mmol) was added as a solid and the reaction stirred for 4 h. Tetraethylammonium bromide (29 mg, 0.14 mmol) was added to the deep orange solution as a solid and stirred for 1 h. Tetraethylammonium cyanide (21 mg, 0.14 mmol) was then added as a solid and the reaction stirred for one hour. Solvent was removed *in vacuo* and the brown-green solid was washed with THF to yield a light green solid. Green, X-ray quality crystals were obtained by vapor diffusion of diethyl ether into DMF (97 mg, 85%).  $^1\text{H}$  NMR ( $\delta$ ,  $\text{CD}_3\text{CN}$ , 300 MHz): 37.41 (br), 12.70 (sh), 10.56 (sh), 5.34 (sh), 3.12 (q, ( $\text{CH}_3\text{-CH}_2$ )<sub>4</sub>N), 1.16 (t, ( $\text{CH}_2\text{-CH}_2$ )<sub>4</sub>N), -7.38 (sh), -15.49 (sh). FTIR (KBr,  $\text{cm}^{-1}$ ):  $\nu(\text{CN})$  2112.  $\mu_{\text{eff}} = 3.25 \mu_{\text{B}}$  (Evan's Method,  $(\text{CD}_3)_2\text{SO}$ , 298 K).  $\lambda_{\text{max}}(e, \text{M}^{-1}\text{cm}^{-1})$  (MeCN): 654(32). Anal. Calcd (found) for  $[\text{Et}_4\text{N}]_2[\text{Ni}(\text{L}^{\text{iPr}})(\text{CN})]$ : C, 66.98 (66.65); H, 8.73 (8.45); N, 11.63 (11.64). Electrochemistry (DMF, 0.2 M  $[\text{n-Bu}_4\text{N}]\text{PF}_6$ )  $E_{1/2} = -251$  mV (vs.  $\text{Fc}/\text{Fc}^+$ ),  $\Delta E_{\text{p}} = 115$  mV,  $i_{\text{pr}}/i_{\text{pr}} = 0.76$ .

### $[\text{Et}_4\text{N}]_3[\text{Ni}(\text{L}^{\text{iPr}})(\mu_2\text{-CN})\text{Co}(\text{L}^{\text{iPr}})]$

To a solution of  $(\text{Et}_4\text{N})_2[\text{NiN}(o\text{-PhNC}(O)^{\text{iPr}})_3\text{CN}]$  (117 mg, 0.14 mmol) in DMF (~ 4 mL) was added  $\text{Et}_4\text{N}[\text{CoN}(o\text{-PhNC}(O)^{\text{iPr}})_3]$  (95 mg, 0.14 mmol) as a DMF solution. After 2 h of stirring, diethyl ether (~ 5 mL) was added to precipitate the product as a reddish-purple solid. The solid was collected by filtration, washed with acetonitrile (~ 5 mL) and diethyl ether (~ 5 mL), and dried *in vacuo* (175 mg, 83%). X-ray quality crystals were grown by slow diffusion of diethyl ether into a concentrated DMF solution of the product.  $^1\text{H}$  NMR ( $\delta$ ,  $(\text{CD}_3)_2\text{SO}$ , 400 MHz): 37.29 (br), 21.25 (br), 20.15 (br), 17.72 (sh), 12.96 (br), 12.65 (sh), 10.68 (sh), 9.34 (br), 7.58 (sh), 6.36 (sh), 5.55 (sh), 3.21 (q, ( $\text{CH}_3\text{-CH}_2$ )<sub>4</sub>N), 1.16 (t, ( $\text{CH}_2\text{-CH}_2$ )<sub>4</sub>N), 0.39 (br), -1.37 (br), -7.16 (sh), -15.68 (sh). FTIR (KBr,  $\text{cm}^{-1}$ ):  $\nu(\text{CN})$  2126.  $\lambda_{\text{max}}(e, \text{M}^{-1}\text{cm}^{-1})$  (DMF): 572(281), 834(40). Anal. Calcd (found) for  $[\text{Et}_4\text{N}]_3[(\text{NiN}(o\text{-PhNC}(O)^{\text{iPr}})_3)(\text{CoN}(o\text{-PhNC}(O)^{\text{iPr}})_3)\text{CN}]$ : C, 66.98 (66.65); H, 8.73 (8.45); N, 11.63 (11.64).

### Cyanide binding to $[\text{Ph}_4\text{P}][\text{Ni}(\text{L}^{\text{iBu}})]$

To an orange solution of  $[\text{Ph}_4\text{P}][\text{Ni}(\text{L}^{\text{iBu}})]$  (41 mg, 0.04 mmol) in acetonitrile (4 mL) was added tetraphenylphosphonium cyanide (16 mg, 0.04 mmol) as a solid and the reaction stirred for one hour. Solvent was removed *in vacuo* and the orange-red solid was washed with THF ( $3 \times 2$  mL) to yield a dark red-orange solid (56 mg, 98%).  $^1\text{H}$  NMR ( $\delta$ ,  $\text{CD}_3\text{CN}$ , 400 MHz): diamagnetic resonances: 8.22, 7.92, 7.75, 7.55, 7.36, 7.22, 7.07, 6.96, 6.78, 6.52, 6.06, 1.27, 1.23, 0.93. paramagnetic resonances: 53.29, 39.49, 30.79, 25.60, 22.16, 21.77, 21.35, 17.02, 14.52, 13.62, 10.13, -1.48, -2.99, -5.04, -18.74, -19.28. FTIR (MeCN,  $\text{cm}^{-1}$ ): 2975, 2868, 2187, 2150, 2109, 1590, 1293, 1224, 1187, 1165, 1110, 763, 725, 693, 529.  $\lambda_{\text{max}}(e, \text{M}^{-1}\text{cm}^{-1})$  (MeCN): 408(sh). Attempts to recrystallize this species afforded only starting materials, *i.e.*,  $[\text{Ph}_4\text{P}][\text{Ni}(\text{L}^{\text{iBu}})]$  and  $\text{PPh}_4[\text{CN}]$ .

### X-ray crystallographic studies

Suitable crystals were coated with Paratone-N oil, suspended on a small fiber loop and placed in a cooled nitrogen gas stream at 173 K on a Bruker D8 APEX II CCD sealed tube diffractometer with graphite monochromated  $\text{Mo-K}\alpha$  (0.71073 Å) radiation. Data were measured using a series of combinations of phi and omega scans with 10 s frame exposures and 0.5° frame widths. Data

collection, indexing and initial cell refinements were all carried out using APEX II software.<sup>51</sup> Frame integration and final cell refinements were done using SAINT software.<sup>79</sup> The final cell parameters were determined from least-squares refinement on 2159 reflections. The structure was solved using Direct methods and difference Fourier techniques (SHELXTL, V6.12).<sup>80</sup> Hydrogen atoms were placed in their expected chemical positions using the HFIX command and were included in the final cycles of least squares refinement using a riding model. All non-hydrogen atoms were refined anisotropically. Scattering factors and anomalous dispersion corrections are taken from the *International Tables for X-ray Crystallography*.<sup>81</sup> Structure solution, refinement, graphics and generation of publication materials were performed using SHELXTL, V6.12 software.<sup>80</sup>

### Magnetic susceptibility measurements

DC magnetic susceptibility data were collected using a Quantum Design MPMS XL SQUID magnetometer at temperatures ranging from 2 to 300 K. Powdered microcrystalline samples were packed in gelatin capsules, inserted into a straw and transported to the magnetometer under dinitrogen. Contributions to the magnetization from the gelatin capsule and the straw were measured independently and subtracted from the total measured signal. Data were corrected for diamagnetic contributions using Pascal's constants. Samples for magnetization measurements were suspended in eicosane to prevent torquing of the crystallites at high magnetic fields. Susceptibility data were fit with theoretical models using a relative error minimization routine (JulX).<sup>72</sup> Attempts to fit magnetization data employed JulX or ANISOFIT 2.<sup>54</sup> Reported coupling constants are based on exchange Hamiltonians of the form  $\hat{H} = -2J(\hat{S}_i \cdot \hat{S}_j)$ .

### Acknowledgements

We thank Rui Cao and Sheri Lense for assistance with X-ray crystallography and Prof. K. S. Hagen for helpful discussions. Leslie A. Alexander is acknowledged for her initial synthesis of [Et<sub>4</sub>N][Ni(L<sup>1Bu</sup>)]. This work was supported by the Emory University Research Council (URC) and the donors of the American Chemical Society Petroleum Research Fund (ACS PRF).

### References

- 1 W. G. Dougherty, K. Rangan, M. J. O'Hagan, G. P. A. Yap and C. G. Riordan, *J. Am. Chem. Soc.*, 2008, **130**, 13510–13511.
- 2 H. J. Kruger, G. Peng and R. H. Holm, *Inorg. Chem.*, 1991, **30**, 734–742.
- 3 J. Shearer and N. Zhao, *Inorg. Chem.*, 2006, **45**, 9637–9639.
- 4 K. P. Neupane and J. Shearer, *Inorg. Chem.*, 2006, **45**, 10552–10566.
- 5 I. Sovago and K. Osz, *Dalton Trans.*, 2006, 3841–3854.
- 6 F. Meyer, E. Kaifer, P. Kircher, K. Heinze and H. Pritzkow, *Chem.–Eur. J.*, 1999, **5**, 1617–1630.
- 7 G. K. Ingle, M. M. Makowska-Grzyka, A. M. Arif and L. M. Berreau, *Eur. J. Inorg. Chem.*, 2007, 5262–5269.
- 8 K. Rudzka, A. M. Arif and L. M. Berreau, *J. Am. Chem. Soc.*, 2006, **128**, 17018–17023.
- 9 E. Kimura, *J. Coord. Chem.*, 1986, **15**, 1–28.
- 10 T. J. Collins, T. R. Nichols and E. S. Uffelman, *J. Am. Chem. Soc.*, 1991, **113**, 4708–4709.
- 11 S. K. Sharma, S. Upreti and R. Gupta, *Eur. J. Inorg. Chem.*, 2007, 3247–3259.
- 12 F. P. Bossu and D. W. Margerum, *Inorg. Chem.*, 1977, **16**, 1210–1214.
- 13 F. P. Bossu and D. W. Margerum, *J. Am. Chem. Soc.*, 1976, **98**, 4003–4004.

- 14 J. Singh, G. Hundal and R. Gupta, *Eur. J. Inorg. Chem.*, 2008, 2052–2063.
- 15 X. Ottenwaelder, A. Aukauloo, Y. Journaux, R. Carrasco, J. Cano, B. Cervera, I. Castro, S. Curreli, M. C. Munoz, A. L. Rosello, B. Soto and R. Ruiz-Garcia, *Dalton Trans.*, 2005, 2516–2526.
- 16 B. Lassalle-Kaiser, R. Guillot, J. Sointon, M.-F. Charlot and A. Aukauloo, *Chem.–Eur. J.*, 2008, **14**, 4307–4317.
- 17 M. Ray, G. P. A. Yap, A. L. Rheingold and A. S. Borovik, *J. Chem. Soc., Chem. Commun.*, 1995, 1777–1778.
- 18 M. Ray, B. Hammes, G. P. A. Yap, A. L. Rheingold and A. S. Borovik, *Inorg. Chem.*, 1998, **37**, 1527–1532.
- 19 B. S. Hammes, D. Ramos-Maldonado, G. P. A. Yap, A. L. Rheingold, V. G. Young and A. S. Borovik, *Coord. Chem. Rev.*, 1998, **174**, 241–253.
- 20 A. V. Lee and L. L. Schafer, *Eur. J. Inorg. Chem.*, 2007, 2245–2255.
- 21 F. P. Bossu, K. L. Chellappa and D. W. Margerum, *J. Am. Chem. Soc.*, 1977, **99**, 2195–2203.
- 22 R. K. Thomson, F. E. Zahariev, Z. Zhang, B. O. Patrick, Y. A. Wang and L. L. Schafer, *Inorg. Chem.*, 2005, **44**, 8680–8689.
- 23 S. Kannan, C. L. Barnes and P. B. Duval, *Chem. Commun.*, 2005, 5997–5998.
- 24 M. Ray, A. P. Golombek, M. P. Hendrich, G. P. A. Yap, L. M. Liable-Sands, A. L. Rheingold and A. S. Borovik, *Inorg. Chem.*, 1999, **38**, 3110–3115.
- 25 B. S. Hammes, D. Ramos-Maldonado, G. P. A. Yap, L. Liable-Sands, A. L. Rheingold, V. G. Young Jr. and A. S. Borovik, *Inorg. Chem.*, 1997, **36**, 3210–3211.
- 26 M. B. Jones and C. E. MacBeth, *Inorg. Chem.*, 2007, **46**, 8117–8119.
- 27 M. B. Jones, K. I. Hardcastle and C. E. MacBeth, *Polyhedron*, 2009, DOI: 10.1016/j.poly.2009.06.013.
- 28 L. Yang, D. R. Powell and R. P. Houser, *Dalton Trans.*, 2007, 955–964.
- 29 D. F. Evans, *J. Chem. Soc.*, 1959, 2003–2005.
- 30 S. K. Sur, *J. Magn. Reson.*, 1989, **82**, 169–173.
- 31 R. S. Drago, *Physical Methods in Chemistry*, W. B. Saunders Company, Philadelphia, 1977.
- 32 M. Ciampolini, *Inorg. Chem.*, 1966, **5**, 35–41.
- 33 A. M. Herrera, R. J. Staples, S. V. Kryatov, A. Y. Nazarenko and E. V. Rybak-Akimova, *Dalton Trans.*, 2003, 846–856.
- 34 L. Sacconi, P. Nannelli, N. Nardi and U. Campigli, *Inorg. Chem.*, 1965, **4**, 943–949.
- 35 B. S. Chohan, S. C. Shoner, J. A. Kovacs and M. J. Maroney, *Inorg. Chem.*, 2004, **43**, 7726–7734.
- 36 L. Banci, C. Benelli and D. Gatteschi, *Inorg. Chem.*, 1984, **23**, 3262–3263.
- 37 M. Mathew and G. J. Palenik, *J. Am. Chem. Soc.*, 1969, **91**, 4923–4924.
- 38 L. Sacconi, M. Ciampolini and G. P. Speroni, *J. Am. Chem. Soc.*, 1965, **87**, 3102–3106.
- 39 K. Nakamoto, *Infrared and Raman Spectra of Inorganic and Coordination Compounds, Fifth Edition*, Wiley, New York, 1997.
- 40 A. W. Addison, T. N. Rao, J. Reedijk, J. Van Rijn and G. C. Verschoor, *J. Chem. Soc., Dalton Trans.*, 1984, 1349–1356.
- 41 K. W. Toernroos, D. Chernyshov, M. Hostettler and H. B. Büergi, *Acta Crystallogr., Sect. C: Cryst. Struct. Commun.*, 2005, **C61**, m450–m452.
- 42 N. Brefuel, C. Duhaion, S. Shova and J.-P. Tuchagues, *Chem. Commun.*, 2007, 5223–5225.
- 43 W. Purcell, S. S. Basson, J. G. Leipoldt, A. Roodt and H. Preston, *Inorg. Chim. Acta*, 1995, **234**, 153–156.
- 44 R. C. Holz and L. C. Thompson, *Inorg. Chem.*, 1993, **32**, 5251–5256.
- 45 M. Palaniandavar, R. J. Butcher and A. W. Addison, *Inorg. Chem.*, 1996, **35**, 467–471.
- 46 A. Lennartson, M. Hakansson and S. Jagner, *New J. Chem.*, 2007, **31**, 344–347.
- 47 K. N. Raymond, P. W. R. Corfield and J. A. Ibers, *Inorg. Chem.*, 1968, **7**, 1362–1372.
- 48 P. A. W. Dean, J. J. Vittal, D. C. Craig and M. L. Scudder, *Inorg. Chem.*, 1998, **37**, 1661–1664.
- 49 S. Pal and A. K. Nandi, *Macromolecules*, 2003, **36**, 8426–8432.
- 50 H. Ma, S. Chattopadhyay, J. L. Petersen and M. P. Jensen, *Inorg. Chem.*, 2008, **47**, 7966–7968.
- 51 L. M. C. Beltran and J. R. Long, *Acc. Chem. Res.*, 2005, **38**, 325–334.
- 52 K. E. Funck, M. G. Hilfiger, C. P. Berlinguette, M. Shatruk, W. Wernsdorfer and K. R. Dunbar, *Inorg. Chem.*, 2009, **48**, 3438–3452.
- 53 C. Zhong, M. Zhao, C. Stern, A. G. M. Barrett and B. M. Hoffman, *Inorg. Chem.*, 2005, **44**, 8272–8276.
- 54 M. P. Shores, J. J. Sokol and J. R. Long, *J. Am. Chem. Soc.*, 2002, **124**, 2279–2292.

- 55 M. Shatruk, C. Avendano and K. R. Dunbar, *Prog. Inorg. Chem.*, 2009, **56**, 155–334.
- 56 K. R. Dunbar and R. A. Heintz, *Prog. Inorg. Chem.*, 1997, **45**, 283–391.
- 57 D. Li, C. Ruschman, S. Parkin, R. Clerac and S. M. Holmes, *Chem. Commun.*, 2006, 4036–4038.
- 58 M. Shatruk, K. E. Chambers, A. V. Prosvirin and K. R. Dunbar, *Inorg. Chem.*, 2007, **46**, 5155–5165.
- 59 A. G. Orpen, L. Brammer, F. H. Allen, O. Kennard, D. G. Watson and R. Taylor, *J. Chem. Soc., Dalton Trans.*, 1989, S1–S83.
- 60 F. Meyer, R. F. Winter and E. Kaifer, *Inorg. Chem.*, 2001, **40**, 4597–4603.
- 61 S. Sarkar, A. Datta, A. Mondal, D. Chopra, J. Ribas, K. K. Rajak, S. M. Sairam and S. K. Pati, *J. Phys. Chem. B*, 2006, **110**, 12–15.
- 62 B. Kersting and G. Steinfeld, *Chem. Commun.*, 2001, 1376–1377.
- 63 M. Gressenbuch and B. Kersting, *Eur. J. Inorg. Chem.*, 2007, 90–102.
- 64 V. Lozan and B. Kersting, *Inorg. Chem.*, 2008, **47**, 5386–5393.
- 65 J. Zinn Paul, N. Sorrell Thomas, R. Powell Douglas, W. Day Victor and A. S. Borovik, *Inorg. Chem.*, 2007, **46**, 10120–10132.
- 66 G. Steinfeld, V. Lozan and B. Kersting, *Angew. Chem., Int. Ed.*, 2003, **42**, 2261–2263.
- 67 M. Gressenbuch, V. Lozan, G. Steinfeld and B. Kersting, *Eur. J. Inorg. Chem.*, 2005, 2223–2234.
- 68 A. D. Bond, S. Derossi, C. J. Harding, E. J. L. McInnes, V. McKee, C. J. McKenzie, J. Nelson and J. Wolowska, *Dalton Trans.*, 2005, 2403–2409.
- 69 T. Lu, X. Zhuang, Y. Li and S. Chen, *J. Am. Chem. Soc.*, 2004, **126**, 4760–4761.
- 70 J. L. Heinrich, P. A. Berseth and J. R. Long, *Chem. Commun.*, 1998, 1231–1232.
- 71 R. Lescouezec, L. M. Toma, J. Vaissermann, M. Verdaguer, F. S. Delgado, C. Ruiz-Perez, F. Lloret and M. Julve, *Coord. Chem. Rev.*, 2005, **249**, 2691–2729.
- 72 E. Bill, *JulX 1.4.1 A Program for the Simulation and Analysis of Magnetic Susceptibility Data*, [http://ewww.mpi-muelheim.mpg.de/bac/logins/bill/julX\\_en.php](http://ewww.mpi-muelheim.mpg.de/bac/logins/bill/julX_en.php).
- 73 W. R. Entley, C. R. Treadway and G. S. Girolami, *Mol. Cryst. Liq. Cryst.*, 1995, **273**, 153–166.
- 74 N. Benbellat, K. S. Gavrilenko, Y. Le Gal, O. Cador, S. Golhen, A. Gouasmia, J.-M. Fabre and L. Ouahab, *Inorg. Chem.*, 2006, **45**, 10440–10442.
- 75 D. Wu, D. Guo, Y. Song, W. Huang, C. Duan, Q. Meng and O. Sato, *Inorg. Chem.*, 2009, **48**, 854–860.
- 76 P. A. Berseth, J. J. Sokol, M. P. Shores, J. L. Heinrich and J. R. Long, *J. Am. Chem. Soc.*, 2000, **122**, 9655–9662.
- 77 F. Karadas, E. J. Schelter, M. Shatruk, A. V. Prosvirin, J. Bacsá, D. Smirnov, A. Ozarowski, J. Krzystek, J. Telsler and K. R. Dunbar, *Inorg. Chem.*, 2008, **47**, 2074–2082.
- 78 F. Gloaguen, J. D. Lawrence, M. Schmidt, S. R. Wilson and T. B. Rauchfuss, *J. Am. Chem. Soc.*, 2001, **123**, 12518–12527.
- 79 *SAINT Version 6.45A*, 2003, Bruker AXS, Inc., Analytical X-ray Systems, 5465 East Cheryl Parkway, Madison WI 53711-5373., 2003.
- 80 G. M. Sheldrick, *Acta Crystallogr., Sect. A: Found. Crystallogr.*, 2008, **A64**, 112–122.
- 81 *International Tables for X-ray Crystallography, Volume C*, A. J. C. Wilson, (ed), Kynoch Academic Publishers, Dordrecht, 1992.